

**Bond angles for O-H defects in SnO<sub>2</sub> from polarization properties of their vibrational modes**Figen Bekisli,<sup>1</sup> W. Beall Fowler,<sup>1</sup> Michael Stavola,<sup>1,\*</sup> Lynn A. Boatner,<sup>2</sup> Erik Spahr,<sup>3</sup> and Gunter Lüpke<sup>3</sup><sup>1</sup>*Department of Physics and the Sherman Fairchild Laboratory, Lehigh University, Bethlehem, Pennsylvania 18015, USA*<sup>2</sup>*Materials Science and Technology Division, Oak Ridge National Laboratory, Oak Ridge, Tennessee 37831, USA*<sup>3</sup>*Department of Applied Science, College of William and Mary, Williamsburg, Virginia 23187, USA*

(Received 12 February 2012; published 3 May 2012)

Infrared absorption experiments made with polarized light yield significant insights into the possible structures of one- and two-O-H defects in SnO<sub>2</sub> that are produced by thermal annealing treatments. These polarized absorption results reveal that a two-O-H defect must involve symmetry-equivalent O-H sites and that the axes of both one- and two-O-H defects are 63°–68° from the *c* axis of the rutile structure. These O-H bond angles found by experiment restrict the microscopic defect structures that are possible and suggest structures associated with either a metal atom substituting for Sn or an interstitial metal atom (such as Sn).

DOI: [10.1103/PhysRevB.85.205202](https://doi.org/10.1103/PhysRevB.85.205202)

PACS number(s): 63.20.Pw, 61.72.Bb, 78.30.Hv

**I. INTRODUCTION**

The transparent conductor SnO<sub>2</sub> has been of technological importance for many years, and recent interest in large-gap semiconductors<sup>1,2</sup> has led to a revival of interest in its fundamental properties. Studies of the origin of *n*-type conduction in SnO<sub>2</sub> suggest the involvement<sup>3,4</sup> of H, which in turn has led to considerations of the detailed structures of H-related defects.<sup>5</sup> The recent infrared (IR) absorption experiments of Bekisli *et al.*<sup>6</sup> have explored the properties of these defects, focusing primarily on the relationship of O-H centers to free-carrier absorption.

When SnO<sub>2</sub> is annealed in an H<sub>2</sub> ambient, two shallow donor centers are formed.<sup>4,6</sup> One shallow donor center is thermally stable up to near 600 °C and has been attributed to H trapped at an O vacancy.<sup>4,6</sup> A second shallow donor center is marginally stable at room temperature and has been assigned to interstitial H with an O-H vibrational line at 3156.1 cm<sup>-1</sup> (Ref. 5). Additional O-H and (O-H)<sub>2</sub> centers are also formed that do not give rise to free carriers.<sup>5,6</sup> (The corresponding deuterium centers have also been investigated.) The hydrogen-related, shallow donor centers can be interconverted between these additional O-H centers by thermal treatments.<sup>6</sup> These interconversion reactions make the conductivity of SnO<sub>2</sub> highly sensitive to its thermal history. What are these additional O-H centers in SnO<sub>2</sub>, and what are their structures? Recent theory has suggested two O-H structures with H trapped at an Sn vacancy as possible candidates.<sup>5</sup>

In this paper, we investigate the polarization properties of the vibrational absorption of O-H centers in SnO<sub>2</sub> that are produced by thermal annealing treatments. SnO<sub>2</sub> has the rutile structure, shown<sup>7</sup> in Fig. 1: Each Sn has six O neighbors, while each O is coplanar with its three Sn neighbors. One O-Sn bond is normal to the *c* axis, while the other two (which are equivalent) make angles of 39.3° and (180°–39.3°) with the +*c* axis.<sup>8</sup> The normal to the plane of O and its three Sn neighbors is itself normal to the *c* axis. As we shall see, this unique crystal structure allows IR polarized absorption experiments and their interpretation to reveal the O-H bond angles of the dominant O-H centers that are formed. These results provide significant insights into the microscopic defect structures that are possible for O-H centers in SnO<sub>2</sub>.

**II. EXPERIMENT**

The SnO<sub>2</sub> samples used in our studies were bulk, rutile phase, single crystals that had been grown by the vapor transport method.<sup>9</sup> To introduce additional hydrogen or deuterium, SnO<sub>2</sub> samples were placed in sealed quartz ampoules filled with H<sub>2</sub> or D<sub>2</sub> gas (2/3 atm at room temperature) and annealed at elevated temperature. The samples were quenched to room temperature in water to terminate the anneals. These treatments in H<sub>2</sub> or D<sub>2</sub> produced an opaque layer of Sn at the sample surface that was removed by lapping and polishing prior to IR absorption experiments. Additional annealing treatments were performed in a conventional tube furnace in an He ambient. The annealing behaviors studied previously have allowed us to select annealing times and temperatures to produce the defects whose structures are to be investigated.<sup>6</sup>

It has been found previously that as-grown SnO<sub>2</sub> contains H impurities.<sup>5,6</sup> To produce an SnO<sub>2</sub> sample that contained primarily D for our studies, an as-grown sample was pre-annealed at 1000 °C for 5 h in an He ambient to remove H. This sample could then be deuterated by annealing in a D<sub>2</sub> ambient as described above.

Infrared absorption spectra were measured with a Bomem DA.3 Fourier-transform-infrared spectrometer that was equipped with a KBr beam splitter and an InSb detector. O-H and O-D vibrational modes were measured in SnO<sub>2</sub> samples held at 4.2 K with a Helitran, continuous-flow cryostat. The IR light was polarized with a wire grid polarizer that was placed after the sample.

**III. POLARIZED ABSORPTION SPECTRA**

Figure 2 shows polarized O-D absorption spectra for an SnO<sub>2</sub> sample into which D had been introduced by annealing in an ambient that contained D<sub>2</sub>. This deuteration treatment was followed by a 30-min anneal at 150 °C in an He ambient to produce the defects of interest. The O-H IR lines that were also seen in this sample resulted from the H that is present in as-grown SnO<sub>2</sub> samples.<sup>5,6</sup> We focus on the polarized O-D spectra because two of the O-H lines of interest were found to overlap, complicating their analysis.<sup>6</sup>

The line at 2360.4 cm<sup>-1</sup> seen for **E**⊥**c** has been assigned to the O-D vibration of interstitial deuterium.<sup>5</sup> The dominant

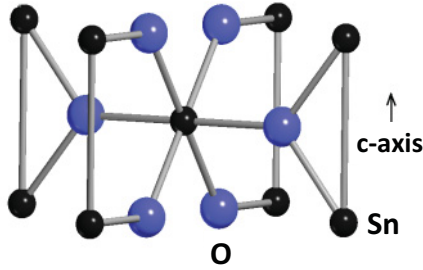


FIG. 1. (Color online) Fragment of the rutile lattice, Ref. 7.

O-D line at  $2425.7\text{ cm}^{-1}$  is seen only for  $\mathbf{E}\perp\mathbf{c}$ , as are several additional weaker O-D lines at  $2432.6$ ,  $2438.5$ , and  $2451.3\text{ cm}^{-1}$ . Unlike its neighbors, the line at  $2446.9\text{ cm}^{-1}$  is seen for both  $\mathbf{E}\perp\mathbf{c}$  and  $\mathbf{E}\parallel\mathbf{c}$ . The line shapes of the  $2446.9\text{ cm}^{-1}$  line for the two polarizations were fit with Gaussian functions to determine their areas. The ratio of these line areas was determined to be  $I_{\parallel}(2446.9)/I_{\perp}(2446.9) = 0.54 \pm 0.05$ .

Figure 2 also shows three lines at  $2477.5$ ,  $2479.7$ , and  $2483.8\text{ cm}^{-1}$  with distinctive polarization properties. The lines at  $2477.5$  and  $2483.8\text{ cm}^{-1}$  were assigned to an  $(\text{O-D})_2$  complex.<sup>6</sup> Figure 3 shows spectra for the O-H and O-D modes that have been attributed to the  $(\text{O-H})_2$  defect and its isotopic siblings. We have carried out a simple mass-and-spring analysis of the  $(\text{O-H})_2$  lines at  $3334.2$  and  $3343.3\text{ cm}^{-1}$ , the corresponding  $(\text{O-D})_2$  lines at  $2477.5$  and  $2483.8\text{ cm}^{-1}$ , and the intermediate lines at  $2479.7$  and  $3339.0\text{ cm}^{-1}$  due to the  $(\text{O-D-H-O})$  center. The small experimental splittings mean that the coupling between the two O-H bonds is weak, so we consider only the harmonic part of this coupling force. While the anharmonicity within each bond is not negligible, it may be calculated from the isotopic data, using the reduced diatomic masses. Then the  $2 \times 2$  harmonic dynamical matrix can be solved, and the force constants can be fit to the harmonic experiment, after which one can add back the anharmonicity.

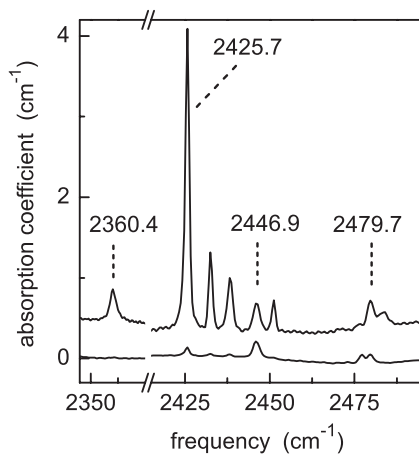


FIG. 2. Infrared absorption spectra ( $T = 4.2\text{ K}$ , resolution =  $1\text{ cm}^{-1}$ ) measured for light polarized with electric vector  $\mathbf{E}\perp\mathbf{c}$  (upper) and  $\mathbf{E}\parallel\mathbf{c}$  (lower) in the O-D region for a sample containing H and D. Here, D was introduced by an anneal (30 min) in  $\text{D}_2$  gas at  $700\text{ }^\circ\text{C}$ . The sample was subsequently annealed for 30 min at  $150\text{ }^\circ\text{C}$  in an He ambient to produce the defects of interest.

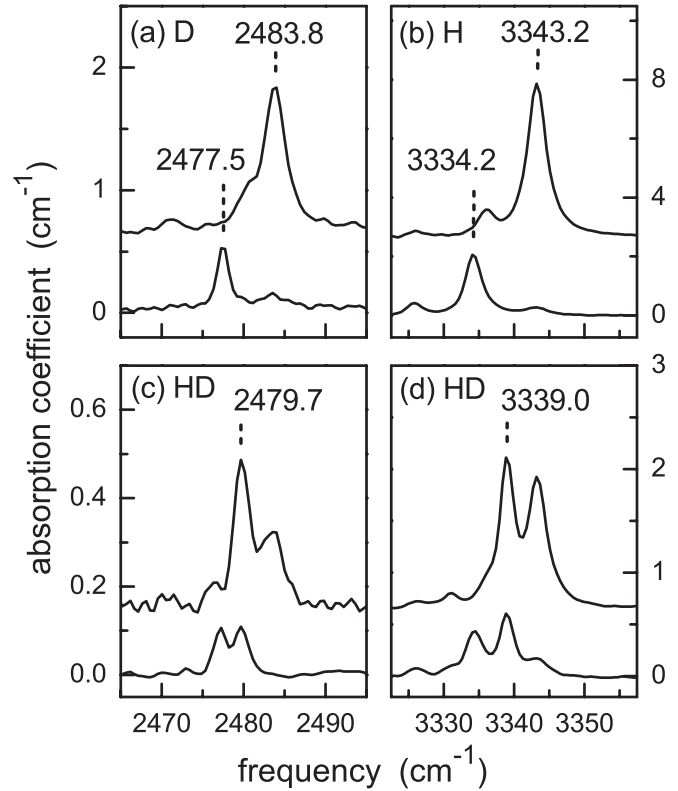


FIG. 3. Infrared absorption spectra ( $T = 4.2\text{ K}$ , resolution =  $1\text{ cm}^{-1}$ ) for O-H and O-D modes in the  $(\text{O-H})_2$  and  $(\text{O-D})_2$  regions measured for light polarized with electric vector  $\mathbf{E}\perp\mathbf{c}$  (upper) and  $\mathbf{E}\parallel\mathbf{c}$  (lower) for samples with different isotopic content. (a) Primarily D, (b) only H, and (c) is  $\text{H} > \text{D}$ . (d) H approximately = D. Here, H or D was introduced into our samples by an anneal (30 min) in  $\text{H}_2$  or  $\text{D}_2$  gas at  $700\text{ }^\circ\text{C}$ . This treatment was followed by an additional anneal between room temperature and  $150\text{ }^\circ\text{C}$  to produce the defects of interest.

This leads to the following results: (1) The two O-H bonds are equivalent; allowing their force constants to differ worsens the agreement with experiment. (2) Using one stretch and one coupling force constant, each of the six experimental frequencies can be fit to within  $0.1\text{ cm}^{-1}$ . (3) The coupling force constant is indeed small, only 0.2% of the stretch force constant. These facts, along with polarization data, are critical clues as to the assignments of the vibrational modes and the likely structure of the  $(\text{O-H})_2$  defect and, by extension, to at least some of the other O-H defects.

The  $(\text{O-D})_2$  and  $(\text{O-H})_2$  lines at  $2483.8$  and  $3343.2\text{ cm}^{-1}$  seen in Figs. 3(a) and 3(b) have  $\mathbf{E}\perp\mathbf{c}$ , while the  $(\text{O-D})_2$  and  $(\text{O-H})_2$  lines at  $2477.5$  and  $3334.2\text{ cm}^{-1}$  have  $\mathbf{E}\parallel\mathbf{c}$ . The O-D and O-H lines at  $2479.7$  and  $3339.0\text{ cm}^{-1}$ , seen in Figs. 3(c) and 3(d) for both parallel and perpendicular polarizations, are assigned to the dynamically decoupled O-D and O-H modes, respectively, of the complex containing both D and H; that is,  $(\text{O-D-H-O})$ .

We have fit the spectra shown in Fig. 3 with sums of Gaussian line shapes in order to determine the relative areas of the overlapping vibrational bands. The ratios of the intensities of the parallel-to-perpendicular polarized modes shown in

Figs. 3(a) and 3(b) are determined to be

$$\begin{aligned} I_{//}(2477.5)/I_{\perp}(2483.8) &= I_{//}(3334.2)/I_{\perp}(3343.2) \\ &= 0.34 \pm 0.05. \end{aligned} \quad (1)$$

The ratios of the intensities of the parallel-to-perpendicular polarizations for the dynamically decoupled modes shown in Figs. 3(c) and 3(d) are determined to be

$$\begin{aligned} I_{//}(2479.7)/I_{\perp}(2479.7) &= I_{//}(3339.0)/I_{\perp}(3339.0) \\ &= 0.4 \pm 0.1. \end{aligned} \quad (2)$$

#### IV. DEFECT MODELS

##### A. O-H bond angles from polarization data

###### 1. Centers containing a single O-H or O-D

Bearing the geometries of rutile in mind, we turn to the observed polarization ratios. Because there are overlapping lines in the O-H spectra around 3282 cm<sup>-1</sup> that are separated in the corresponding O-D spectra around 2447 cm<sup>-1</sup>, in that range, we use the latter for analysis (Fig. 2). From the rutile symmetry and the equivalence of different oxygen sites, the ratio of parallel-to-perpendicular intensities for an O-D transition dipole that makes an angle  $\theta$  with respect to the  $c$  axis is given by

$$I_{//}/I_{\perp} = 2\cot^2(\theta). \quad (3)$$

All but two of the observed O-D lines (Fig. 2) show absorption only for polarization perpendicular to the  $c$  axis; hence, for these lines  $\theta = 90^\circ$ , and their transition dipoles are normal to the  $c$  axis. The ratio of parallel-to-perpendicular polarization of  $0.54 \pm 0.05$  for the O-D line at 2446.9 cm<sup>-1</sup> leads to an O-D angle of  $63^\circ$  or  $(180^\circ - 63^\circ) \pm 1^\circ$  from the  $+c$  axis.

###### 2. Centers containing two O-H or O-D

The O-D bond angles for the (O-D)<sub>2</sub> center whose lines are at 2477.5 and 2483.8 cm<sup>-1</sup> can be determined from our polarization data, and similarly for the (O-H)<sub>2</sub> center whose lines are at 3334.2 and 3343.2 cm<sup>-1</sup>. In this case, the polarization ratio given in Eq. (1) leads to an O-D (or O-H) bond angle of  $68^\circ$  or  $(180^\circ - 68^\circ) \pm 2^\circ$  from the  $+c$  axis for the (O-D)<sub>2</sub> [or (O-H)<sub>2</sub>] center.

The polarization ratios for the dynamically decoupled O-D and O-H modes of the (O-D-H-O) center at 2479.7 and 3339.0 cm<sup>-1</sup> provide a consistency check of the bond angle determined for the (O-D)<sub>2</sub> complex. The polarization ratio for the dynamically decoupled O-D mode given in Eq. (2) leads to an O-D bond angle of  $66^\circ$  or  $(180^\circ - 66^\circ) \pm 3^\circ$ , and similarly for O-H. This result agrees with the value determined for the (O-D)<sub>2</sub> center to within experimental error.

##### B. Microscopic defect structures

The polarization data presented here provide constraints on possible defect models. These defects must involve perturbed O-H for which the perturbation causes only a modest

displacement of the bond away from the normal to the  $c$  axis. Furthermore, the perturbation must be such that, in the (O-H)<sub>2</sub> case, the two O-H bonds are equivalent.

Hlaing Oo *et al.*<sup>5</sup> have reported calculations on H trapped at an Sn vacancy and suggest that the 3261.7 and 3282.0 cm<sup>-1</sup> lines are associated with this defect. (These would correspond to the 2425.7 and 2446.9 cm<sup>-1</sup> O-D lines.) Because of the symmetry of the Sn vacancy, there will indeed be two inequivalent types of O-H sites. They find the O-H bond perpendicular to the  $c$  axis (denoted as axial by Hlaing Oo *et al.*) to be less stable than the other (equatorial) by  $\sim 0.1$  eV, and they attribute the 3261.7 cm<sup>-1</sup> line to the equatorial configuration and the 3282.0 line to the axial configuration. However, Hlaing Oo *et al.* did not have access to the polarization data reported here that provide structure-sensitive clues to what IR line assignments or defect structures might be possible.

The attributions proposed by Hlaing Oo *et al.*<sup>5</sup> are not consistent with our polarization data. First, we find the lower-energy line to be polarized perpendicular to the  $c$  axis and thus attributable to an O-H bond in the axial direction, while the higher-energy line has some polarization parallel to the  $c$  axis and thus might be a candidate for an equatorial defect. Further reflection, however, makes the assignment of H at an Sn vacancy problematic, as the O-H equatorial bond would be expected to be near the corresponding O-Sn direction, or  $\sim 30^\circ - 40^\circ$  with the  $+c$  axis. This, in turn, would predict a ratio of parallel-to-perpendicular polarization intensities [Eq. (3)] of  $\sim 3$  to 6, a factor of 6 to 12 larger than observed. Similar problems arise for the assignment of the (O-H)<sub>2</sub> defect: while equivalent O-H sites exist, the same bond angle problem would occur. We conclude, therefore, that while the axial O-H associated with the Sn vacancy could be the origin of one of the observed transitions with polarization perpendicular to  $c$ , there is no spectroscopic evidence for the existence of the equatorial configuration or for an Sn-vacancy-associated (O-H)<sub>2</sub> defect.

Besides the Sn vacancy, the other two intrinsic lattice defects that have been considered to exist<sup>4,10</sup> in SnO<sub>2</sub> are the O vacancy and the Sn interstitial. In the rutile lattice, one or two interstitial H attached to one or two O next to either the O vacancy or the Sn interstitial could satisfy the symmetry requirements indicated above. Figure 4 shows how this could happen in the case of an Sn interstitial. The vibration of a single H attached to O(1), with the same  $c$ -axis value as the Sn interstitial, would have polarization perpendicular to the

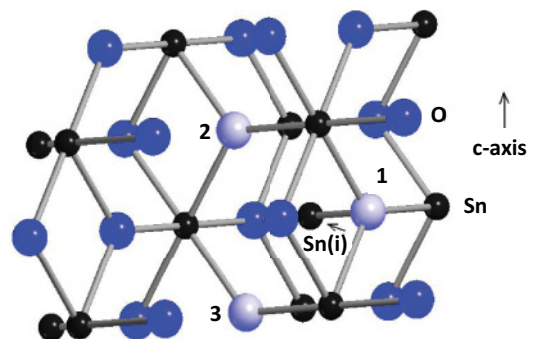


FIG. 4. (Color online) Schematic portion of SnO<sub>2</sub> containing an Sn interstitial. Special neighboring oxygens are labeled 1–3, Ref. 7.

$c$  axis, while if the H were one plane higher or lower, attached to O(2) or O(3), the symmetry breaking due to the presence of the Sn interstitial could lead to a small relaxation of the H along the  $c$  direction, and consequently both distinct parallel and perpendicular polarizations would occur. Additionally, two H trapped, one on O(2) and the other on O(3), would be equivalent and again could have some  $c$ -axis relaxation, and consequently both polarizations would occur. Other two-H defects involving more distant O (and H) might also exist.

It seems highly unlikely that an interstitial H adjacent to an O vacancy would remain interstitial, rather than vacancy centered. Thus, the most likely intrinsic defect accompanying interstitial H would be the Sn interstitial. Unpublished calculations<sup>11</sup> based on this model using the CRYSTAL06 code<sup>12</sup> support this notion as well as the issues raised above with the Sn vacancy model.

## V. CONCLUSIONS

The combination of structure-sensitive polarization data and a mass-and-spring analysis cast doubt upon a model involving H trapped at an Sn vacancy,<sup>5</sup> but are consistent with the notion that several of the O-H and O-D lines seen in SnO<sub>2</sub> could be associated with one or two H or D trapped next to an Sn interstitial. Namely, the O-H/O-D pair at 3261.5/2425.7 cm<sup>-1</sup> could arise from an H or D trapped at O(1) in Fig. 4, the pair at 3281.8/2446.9 could arise from an H or D trapped at O(2) or O(3), and the lines in the region 3340/2480 cm<sup>-1</sup> could arise from two H or D trapped at O(2) and O(3).

The symmetry constraints imposed by these data could also be satisfied by hydrogens trapped near either a substitutional or an interstitial impurity metal atom. Given some question about

the formation energy of interstitial Sn (Kiliç and Zunger<sup>10</sup> predicted a low formation energy for interstitial Sn, while Singh *et al.*<sup>4</sup> found the opposite), these alternatives bear consideration. We believe the impurity alternatives are unlikely for several reasons. First, similar spectra arise in samples obtained from different sources.<sup>5,6</sup> Second, impurities that are associated with O-H bands in cassiterite<sup>13</sup> lead to absorption bands that are absent in our samples. However, at present, this possibility cannot be totally ruled out.

As noted earlier, we believe that the only possible observed O-H absorption associated with the Sn vacancy would arise from a single axial O-H. This indeed could be the source of one of the bands still unassigned in the spectrum, e.g. one of the lines between 2425.7 and 2451.3 cm<sup>-1</sup> for O-D. We note, however, that because the nature of this O-H bond is quite different from the interstitial H-substitutional O bond, it would be coincidental if its vibration would lie among those characterized by the latter. Alternatively, the unassigned bands could arise from H trapped near but not at the Sn interstitial. Further experimental and theoretical work may settle some of these remaining issues. In particular, calculations of vibrational frequencies for the proposed complexes would be useful.

## ACKNOWLEDGMENTS

We thank Haoxiang Zhang for his help in the preparation of samples. This work was supported by NSF Grants DMR-0802278 and DMR-1160756. M.S. is grateful for an Award for Senior US Scientists from the Humboldt Foundation. Research at the Oak Ridge National Laboratory for one author (L.A.B.) is sponsored by the US Department of Energy, Basic Energy Sciences, Materials Science and Technology Division.

\*mjsa@lehigh.edu

<sup>1</sup>H. L. Hartnagel, A. L. Dawar, A. K. Jain, and C. Jagadish, *Semiconducting Transparent Thin Films* (Institute of Physics, London, 1995).

<sup>2</sup>*Transparent Electronics: From Synthesis to Applications*, edited by A. Facchetti and T. Marks (Wiley, New York, 2010).

<sup>3</sup>C. Kiliç and A. Zunger, *Appl. Phys. Lett.* **81**, 73 (2002).

<sup>4</sup>A. K. Singh, A. Janotti, M. Scheffler, and C. G. Van de Walle, *Phys. Rev. Lett.* **101**, 055502 (2008).

<sup>5</sup>W. M. Hlaing Oo, S. Tabatabaei, M. D. McCluskey, J. B. Varley, A. Janotti, and C. G. Van de Walle, *Phys. Rev. B* **82**, 193201 (2010).

<sup>6</sup>F. Bekisli, M. Stavola, W. B. Fowler, L. Boatner, E. J. Spahr, and G. Lüpke, *Phys. Rev. B* **84**, 035213 (2011).

<sup>7</sup>P. Ugliengo, D. Viterbo, and G. Chiari, *Z. Kristallogr.* **207**, 9 (1993); P. Ugliengo, *MOLDRAW: A program to display and manipulate molecular and crystal structures*, Torino, 2006, available at [<http://www.moldraw.unito.it>].

<sup>8</sup>B. Thiel and R. Helbig, *J. Cryst. Growth* **32**, 259 (1976).

<sup>9</sup>A. A. Bolzan, C. Fong, B. J. Kennedy, and C. J. Howard, *Acta Cryst.* **B53**, 373 (1997).

<sup>10</sup>C. Kiliç and A. Zunger, *Phys. Rev. Lett.* **88**, 095501 (2002).

<sup>11</sup>W. B. Fowler, F. Bekisli, and M. J. Stavola (unpublished).

<sup>12</sup>R. Dovesi, V. R. Saunders, C. Roetti, R. Orlando, C. M. Zicovich-Wilson, F. Pascale, B. Civalleri, K. Doll, N. M. Harrison, I. J. Bush, Ph. D'Arco, and M. Llunell, *Crystal06 User's Manual* (University of Torino, Torino, 2006).

<sup>13</sup>Z. Losos and A. Beran, *Mineral Petrol* **81**, 219 (2004).